ChemComm

COMMUNICATION

View Article Online
View Journal | View Issue

Cite this: *Chem. Commun.*, 2026, **62**, 5477

Received 16th October 2025,
Accepted 10th February 2026

DOI: 10.1039/d5cc05918f

rsc.li/chemcomm

Base-catalyzed switchable reactivity of *N*-acyl-α-aminonitriles: oxidative decyanation to imides and hydrolysis to amides in batch and flow conditions

Vikraman Ganesh Moorthi,[a] Vijay Thavasianandam Seenivasan,[b] Sharmila Nokku,[a] Aron Manick Joel,[a] Wei-Yu Lin *[b] and Gopal Chandru Senadi *[ab]

A base-catalyzed, transition-metal-free synthesis of imides and amides from *N*-acyl-α-aminonitriles is reported under batch and continuous-flow conditions. Imides are selectively formed in the presence of open air or an O_2 atmosphere, while degassed H_2O–DMSO conditions afford amides. The protocol shows good scalability and broad functional-group tolerance, and enables late-stage modification of pharmaceutically relevant, ibuprofen-derived substrates; mechanistic studies suggest oxidative decyanation and nitrile hydrolysis pathways for imides and amides, respectively.

The imide functional group is a key structural motif prevalent in numerous natural products and widely exploited in pharmaceuticals[1a,b] and materials science.[1c] Representative examples include penimide A, a fungitoxic natural product,[2a] berkeleyamide B,[2b] and approved drugs such as dermagen (a skin-care agent),[2c] fumaramidmycin (an antibiotic),[2d] and aniracetam (a cognitive enhancer),[2e] all defined by the imide scaffold (Fig. 1). Its broad utility in bioactive molecules and materials continues to drive the development of efficient and practical synthetic strategies for imide scaffolds.[3]

Classical approaches to imide synthesis primarily include the Mumm rearrangement, which involves a 1,3-(O–N) acyl transfer from an acyl imidate to an imide (Scheme 1a),[4] and the direct acylation of amides with acid chlorides, anhydrides, or isocyanates (Scheme 1b).[5] While effective, these strategies often rely on toxic reagents and generate significant chemical waste. To address these limitations, Bode and co-workers developed a chemoselective acylation of amides with potassium acyltrifluoroborates (KATs) under aqueous acidic conditions.[6] In addition, a wide range of modern strategies for imide formation have emerged, including palladium-catalyzed aminocarbonylations, dicarbonylation of amines, hydroamidocarbonylation of olefins, and radical oxidative carbonylations (Scheme 1c),[7] as well as oxidative cross-coupling (Scheme 1d),[8] α-oxygenation (Scheme 1e),[9] isocyanide-based multi-component reactions,[10] visible-light and electrochemical approaches,[11,12] and a few other notable methods.[13] Despite these advances, many of these methodologies still depend on transition-metals, stoichiometric oxidants, or complex setups, which can restrict their practicality and broader synthetic applicability. This highlights the continued need for efficient, sustainable, and operationally simple approaches for imide synthesis. The motivation for this work arose from studies on the base-promoted Nef reaction (Scheme 1f)[14] and the oxidative amidation of α-substituted malonitriles (Scheme 1g)[15] using molecular oxygen, along with our ongoing investigations on α-aminonitriles.[16a–c] Herein, we report a base-catalyzed, condition-switchable strategy that enables oxidative imidation *via* decyanation or amide formation *via* nitrile hydrolysis under both batch and continuous-flow conditions (Schemes 1h and 1i).

Initial screening of model substrate **1a** with Et_3N delivered **2a**, albeit in only 15% yield, whereas DBU gave a markedly improved 83% yield (Table 1, entries 1 and 2). To further enhance the efficiency, a range of bases was evaluated and Cs_2CO_3 emerged as the most effective, affording **2a** in 87% yield, while DIPEA, DMAN, K_2CO_3, Na_2CO_3 and $NaHCO_3$ were

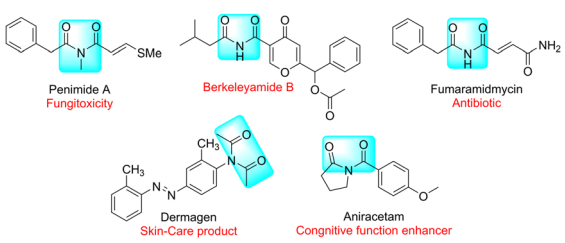

Fig. 1 Representative examples of imides found in natural products and marketed drugs.

[a] *Green and Sustainable Synthesis Laboratory, Department of Chemistry, College of Engineering and Technology, SRM Institute of Science and Technology, SRM Nagar, Kattankulathur - 603 203, Chengalpattu District, Tamil Nadu, India. E-mail: chandrug@srmist.edu.in*

[b] *Department of Medicinal and Applied Chemistry, Kaohsiung Medical University, Kaohsiung, Taiwan. E-mail: wylin@kmu.edu.tw*

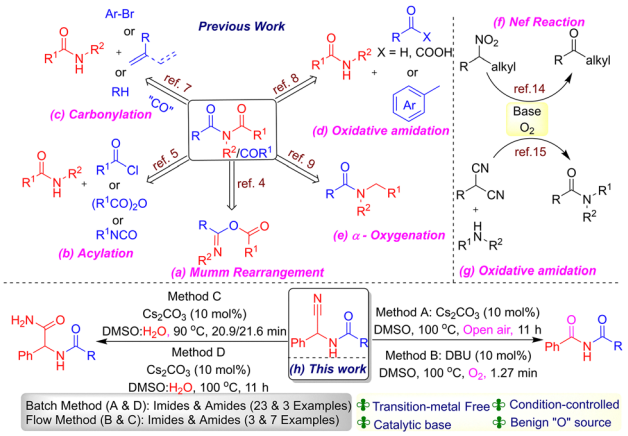

Scheme 1 Reported approaches to imide synthesis and this work.

Table 1 Optimization of the reaction parameters for the synthesis of imides[ab]

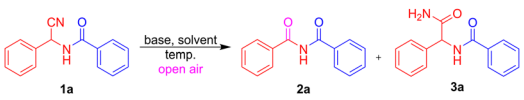

Entry	Base (x mol%)	Solvent	Temp. (°C)	Yield[b] (%) (**2a**/**3a**)
1	Et_3N (10)	DMSO	100	15/0
2	DBU (10)	DMSO	100	83/0
3	DIPEA (10)	DMSO	100	23/0
4	DMAN (10)	DMSO	100	56/0
5	K_2CO_3 (10)	DMSO	100	72/0
6	Na_2CO_3 (10)	DMSO	100	76/0
7	$NaHCO_3$ (10)	DMSO	100	85/0
8	**Cs_2CO_3 (10)**	**DMSO**	**100**	**87/0**
9	Cs_2CO_3 (10)	EtOH	75	N.R.
10	Cs_2CO_3 (10)	1,4-Dioxane	100	21/0
11	Cs_2CO_3 (10)	ACN	80	16/0
12	Cs_2CO_3 (10)	H_2O : DMSO (8 : 2)	100	57/25
13[c]	Cs_2CO_3 (10)	H_2O : DMSO (8 : 2)	100	0/78[d]
14	Cs_2CO_3 (20)	DMSO	100	83/0
15	Cs_2CO_3 (05)	DMSO	100	68/0
16	Cs_2CO_3 (10)	DMSO	80	64/0
17	Cs_2CO_3 (10)	DMSO	120	79/0
18[e]	Cs_2CO_3 (10)	DMSO	100	23/0
19[f]	Cs_2CO_3 (10)	DMSO	100	85/0

[a] Reaction conditions: All reactions were carried out using **1a** (0.5 mmol), base (x, mol%), and solvent (0.15 M) in a vial at the indicated temperature for 11 h under open air. [b] Isolated yield. [c] N_2 degassed, then sealed. [d] Yield is based on recovered starting material. [e] Ar atmosphere. [f] O_2 atmosphere. Abbreviations: DBU (1,8-diazabicyclo[5.4.0]undec-7-ene). DIPEA (*N*,*N*-diisopropylethylamine). DMAN (1,8-bis(dimethylamino)naphthalene). DMSO (dimethyl sulfoxide). EtOH (ethanol). ACN (acetonitrile). N.R. (no reaction).

less competent (Table 1, entries 3–8). Examination of the solvent effects revealed that EtOH, 1,4-dioxane and ACN were inferior to DMSO (Table 1, entries 9–11). However, using H_2O : DMSO (8 : 2) (Table 1, entry 12), as the solvent, the expected product **2a** was obtained in 57% yield, along with the nitrile-hydrolyzed product **3a** in 25% yield. To improve the selectivity toward **3a**, the reaction conditions were slightly modified. The mixture was degassed under N_2 and then sealed (Table 1, entry 13), resulting in the selective formation of **3a** in 78% yield, and the unreacted starting material was recovered. Variation of the catalyst loading showed that lowering Cs_2CO_3 reduced the yield, whereas increasing it to 20 mol% provided no additional benefit (Table 1, entries 14 and 15). Temperature optimization established 100 °C as optimal, with diminished efficiency at 80 °C and no improvement at 120 °C (Table 1, entries 16 and 17). Variation of the reaction atmosphere revealed the crucial role of air, as the yield dropped to 23% under Ar and showed no significant change under O_2 (Table 1, entries 18 and 19). Taken together, these studies defined the optimal conditions as 10 mol% Cs_2CO_3 in DMSO (0.15 M) at 100 °C under open air, which were then employed in subsequent scope studies for imides.

The synthetic scope of the *N*-acyl-α-aminonitrile framework was comprehensively investigated (Table 2) by systematically varying the substituents, demonstrating broad applicability for oxidative decyanation reactions. Initial exploration focused on the phenyl group, revealing that electron-donating substituents such as 3-Me (**1b**), 4-Me (**1c**), 3-MeO (**1d**), 4-MeO (**1e**), and 3,4,5-tri-MeO (**1f**) successfully afforded the desired imide products **2b**–**2f** in good to excellent yields, ranging from 57% to 83%. Subsequently, halogen-substituted derivatives, including 4-F (**1g**), 4-Cl (**1h**), 4-Br (**1i**), and 3,4,5-tri-F (**1j**), also yielded the corresponding imides **2g**–**2j** with satisfactory yields (52% to 74%). The methodology was further extended to electron-withdrawing groups such as 4-CF_3 (**1k**), 4-CN (**1l**), and 4-NO_2 (**1m**), which underwent oxidative decyanation to produce **2k**–**2m** in 48% to 63% yields under standard conditions. To enhance the versatility of the reaction, diverse aromatic and heteroaromatic systems including 2-naphthyl (**1n**), benzyl (**1o**), 2-furyl (**1p**),

Table 2 Cs_2CO_3-catalyzed oxidative imidation of *N*-acyl-α-aminonitriles[ab]

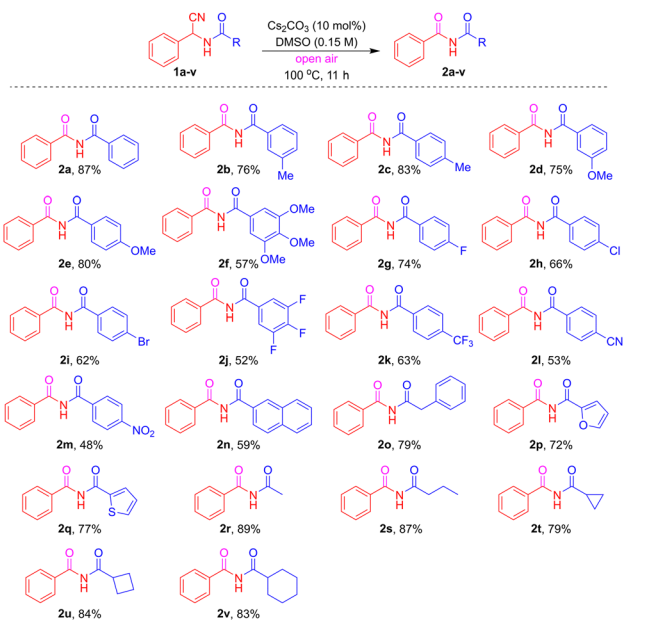

[a] Reaction conditions: Compound **1a**–**v** (0.5 mmol) and Cs_2CO_3 (10 mol%) in DMSO (0.15 M) were stirred in open air at 100 °C for 11 h. [b] Isolated yields.

and 2-thiophenyl (**1q**) were successfully converted into their respective imides **2n**–**2q**, with yields ranging from 59% to 79%. Remarkably, the scope of the R-functionality was extensively evaluated with various linear and cyclic aliphatic derivatives, such as methyl (**1r**), *n*-propyl (**1s**), cyclopropyl (**1t**), cyclobutyl (**1u**), and cyclohexyl (**1v**), all of which afforded the desired compounds **2r**–**2v** in good to excellent yields, specifically 79% to 89%. Notably, aliphatic derivatives generally demonstrated superior yields compared to their aromatic and heteroaromatic counterparts. Similarly, to extend the scope, the reaction conditions described in Table 1, entry 13, were tested for other representative derivatives (**1a**, **1b**, **1d**, **1l** and **1o**) to afford the nitrile hydrolysis products amides (see the SI, 2.5).

Enhanced mass and heat transfer in a microtubing flow reactor[17] significantly accelerated the reaction; however, under flow conditions using catalytic Cs_2CO_3 in H_2O–DMSO (8 : 2) in the presence of O_2, a mixture of imide **2a** and amide **3a** was obtained in 25% and 37% yield, respectively (see the SI, 2.6). The formation of the amide is likely attributable to the presence of water used to dissolve Cs_2CO_3. To suppress amide formation, the next best conditions identified in Table 1 (entry 2) were employed, affording the desired imide **2a** in 87% yield within a residence time of 1.27 min. The protocol was extended to substrates bearing a 4-Me substituent (**1c**) and a 4-Cl substituent (**1h**), delivering the corresponding imides in 65% and 51% yield, respectively (see the SI, 2.7). Unreacted starting material was recovered, and yields are reported based on recovered starting material; further increases in residence time were not explored. Furthermore, to improve the selectivity toward amide **3a**, a systematic optimization in the absence of O_2 (see the SI, Table S1) delivered amide **3a** in 76% yield using flow rates (F_1 = 20 μL min^{-1}, F_2 = 40 μL min^{-1}) at 90 °C with a residence time of 20.9 min. The scope was further extended to electron-donating, halogen-substituted, electron-withdrawing, benzyl and heteroaryl substrates and all of them gave better yields in shorter reaction times as compared to the batch amide synthesis (Scheme 2).

To demonstrate scalability, gram-scale reactions were performed under the optimized conditions (Scheme 3a). The model substrate **1a** (1.0 g) afforded imide **2a** in 82% yield, while aliphatic (**1s** to **2s**, 85%) and heteroaryl (**1q** to **2q**, 72%) substrates also delivered good yields. Late-stage modification of a pharmaceutically relevant, ibuprofen-derived substrate furnished imide (**1w** to **2w**) in 73% yield, further demonstrating the robustness of the protocol (Scheme 3b). Mechanistic studies revealed no product in the absence of base (Scheme 3c), and product suppression with TEMPO and TEMPOL suggested a radical pathway (Scheme 3d). $H_2{}^{18}O$-labeling experiments were conducted to probe oxygen incorporation in products **2a** (batch) and **3a** (flow). LC–MS analysis revealed no ^{18}O incorporation in imide **2a** (Scheme 3e), whereas clear incorporation of ^{18}O was observed in the amide product **3a** (Scheme 3f) (see the SI, 10).

Furthermore, to verify the involvement of superoxide anion radicals in the formation of acyclic imides, we carried out room-temperature EPR studies (X-band, 9.65 GHz) using DMPO (0.1 mol L^{-1}) as a spin trap (see the SI, Fig. S4). Spectra were recorded under three conditions: (i) DMPO in DMSO, (ii) DMPO with substrate **1a** and base in DMSO, and (iii) DMPO with substrate **1a** in DMSO. In the stacked spectra, the signal marked (*) corresponds to DMPO, while the feature labeled (Φ) arises from its oxidized adduct, consistent with the trapping of superoxide species. The characteristic hyperfine pattern together with a *g* value of 2.0035 provides strong evidence for the generation of superoxide under the reaction conditions.[18]

Based on control experiments, a plausible reaction mechanism is proposed (Scheme 4).[16] Under basic conditions, deprotonation of *N*-acyl α-aminonitrile **1** generates the amidyl anion **A**, which undergoes a rapid [1,2]-H shift to afford the carbanion **B**. The latter engages in a single-electron transfer (SET) with

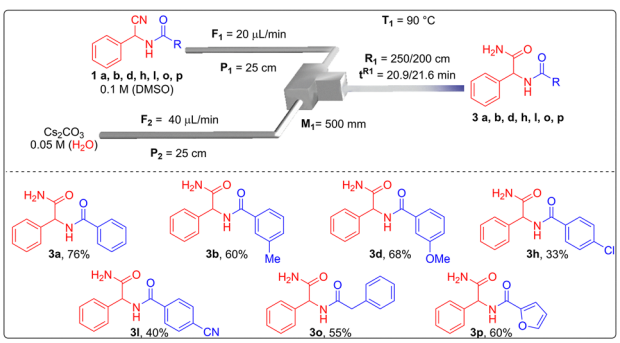

Scheme 2 Continuous-flow approach for the hydrolysis of *N*-acyl α-aminonitriles to amides.

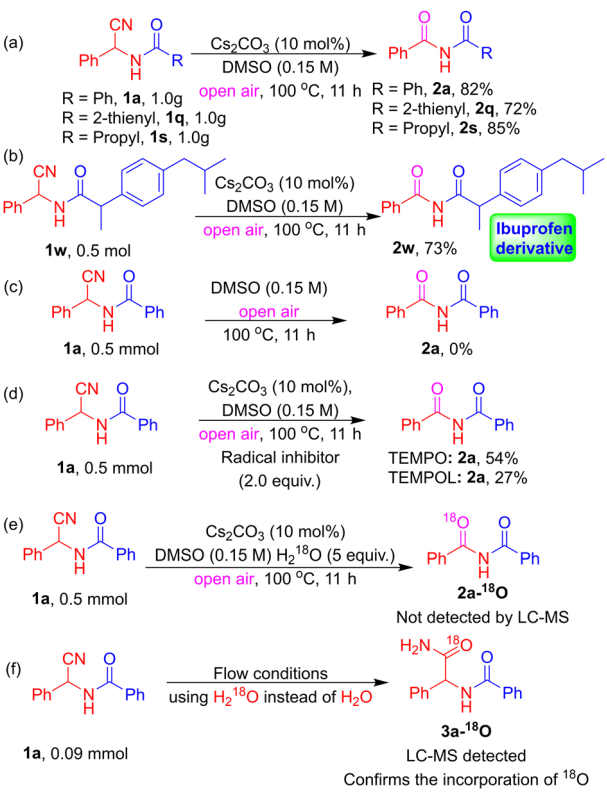

Scheme 3 Synthetic applications and control studies.

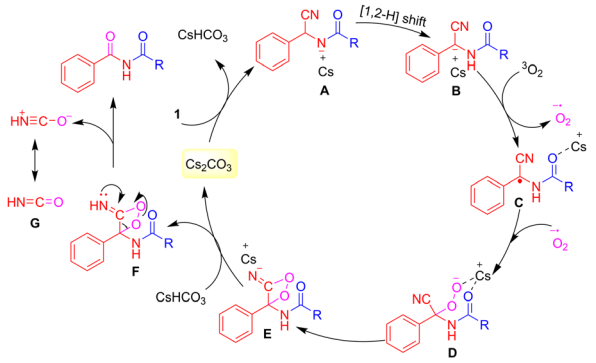

Scheme 4 Plausible reaction mechanism.

molecular oxygen to produce radical intermediate **C** and a superoxide radical anion. Coupling of **C** with the superoxide species forms the peroxy intermediate **D**, which undergoes intramolecular cyclization to give the imino-dioxetane **E**. Proton transfer from **E** furnishes intermediate **F**, and subsequent C–C bond cleavage releases isocyanic acid **G**, affording the acyclic imide **2**. On the other hand, the α-carbanion **B** undergoes delocalization into the nitrile group, giving a resonance-stabilized ketenimine intermediate **II**, which reacts with water to afford the iminol species **III**. Subsequent enol–keto tautomerization of **III** furnishes the corresponding amide product **3** (see the SI, Scheme S1).

In summary, a base-catalyzed, condition-switchable protocol enables the transformation of *N*-acyl-α-aminonitriles into imides or amides under both batch and continuous-flow conditions. Flow processing allows access to both product classes with significantly shorter residence times compared to batch reactions. Mechanistic investigations indicate that the carbonyl oxygen in the amide product originates from water, as demonstrated by $H_2{}^{18}O$-labeling experiments, while radical inhibition and EPR studies support a radical pathway involving superoxide species for imide formation. The practicality of the method is demonstrated through gram-scale synthesis and late-stage modification of an ibuprofen-derived substrate. Further studies aimed at expanding the synthetic utility of *N*-acyl-α-aminonitriles are ongoing.

V. G. M., S. N., and A. M. J., thank the SRM Institute of Science and Technology for the PhD fellowship. Dr G. C. S. acknowledges Anusandhan National Research Foundation (ANRF) for the Core Research Grant (File No. CRG/2022/006963). The authors thank IIISM, SRM Institute of Science and Technology, for providing an NMR facility. The authors also thank the Department of Chemistry, SRM Institute of Science and Technology, for providing the HRMS facilities. The authors also thank the Centre for Research Resources and Development, Kaohsiung Medical University, for 400 MHz NMR and LC–MS analyses. The authors further acknowledge the Academia Sinica Small Molecule Mass Spectrometry Facility for mass spectrometric analyses.

Conflicts of interest

There are no conflicts to declare.

Data availability

The supporting data have been provided as part of the supplementary information (SI). Supplementary information: Table S1, Scheme S1, and Fig. S1–S145. NMR spectra and further experimental details. See DOI: https://doi.org/10.1039/d5cc05918f.

References

1 (*a*) L. Raj, T. Ide, A. U. Gurkar, M. Foley, M. Schenone, X. Li, N. J. Tolliday, T. R. Golub, S. A. Carr, A. F. Shamji, A. M. Stern, A. Mandinova, S. L. Schreiber and S. W. Lee, *Nature*, 2011, **475**, 231–234; (*b*) M. Prudhomme, *Eur. J. Med. Chem.*, 2003, **38**, 123–140; (*c*) Z. Cheng, X. Zhu, E. T. Kang and K. G. Neoh, *Macromolecules*, 2006, **39**, 1660–1663.
2 (*a*) T. Pacher, A. Raninger, E. Lorbeer, L. Brecker, P. P.-H. But and H. Greger, *J. Nat. Prod.*, 2010, **73**, 1389–1393; (*b*) A. A. Stierle, D. B. Stierle and B. Patacini, *J. Nat. Prod.*, 2008, **71**, 856–860; (*c*) D. Vacher, *Ann. Pharm. Fr.*, 2005, **63**, 207–210; (*d*) H. B. Maruyama, Y. Suhara, J. S. Watanabe, Y. Maeshima, N. Shimizu, M. O. Hamada, H. Fujimoto and K. Takano, *J. Antibiot.*, 1975, **28**, 636–647; (*e*) K. Nakamura, *CNS Drug Rev.*, 2006, **8**, 70–89.
3 J. Sperry, *Synthesis*, 2011, 3569–3580.
4 O. Mumm, H. Hesse and H. Volquartz, *Chem. Ber.*, 1915, **48**, 379–391.
5 (*a*) Q. E. Thompson, *J. Am. Chem. Soc.*, 1951, **73**, 5841–5846; (*b*) C. D. Hurd and A. G. Prapas, *J. Org. Chem.*, 1959, **24**, 388–392.
6 A. O. Gálvez, C. P. Schaack, H. Noda and J. W. Bode, *J. Am. Chem. Soc.*, 2017, **139**, 1826–1829.
7 (*a*) A. Schnyder and A. F. Indolese, *J. Org. Chem.*, 2002, **67**, 594–597; (*b*) H. Li, K. Dong, H. Neumann and M. Beller, *Angew. Chem., Int. Ed.*, 2015, **127**, 10377–10381; (*c*) H. Li, X. Fang, R. Jackstell, H. Neumann and M. Beller, *Chem. Commun.*, 2016, **52**, 7142–7145; (*d*) C.-S. Kuai, L.-C. Wang, J.-X. Xu and X.-F. Wu, *Org. Lett.*, 2022, **24**, 451–456; (*e*) L. Lu, D. Cheng, Y. Zhan, R. Shi, C.-W. Chiang and A. Lei, *Chem. Commun.*, 2017, **53**, 6852–6855.
8 (*a*) H. Jiang, A. Lin, C. Zhu and Y. Cheng, *Chem. Commun.*, 2013, **49**, 819–821; (*b*) J. Wang, C. Liu, J. Yuan and A. Lei, *Chem. Commun.*, 2014, **50**, 4736–4739; (*c*) N. Xu, J. Liu, D. Li and L. Wang, *Org. Biomol. Chem.*, 2016, **14**, 4749–4757; (*d*) H. Aruri, U. Singh, S. Kumar, M. Kushwaha, A. P. Gupta, R. A. Vishwakarma and P. P. Singh, *Org. Lett.*, 2016, **18**, 3638–3641.
9 (*a*) L. Xu, S. Zhang and M. L. Trudell, *Chem. Commun.*, 2004, 1668–1669; (*b*) K. C. Nicolaou and C. J. N. Mathison, *Angew. Chem., Int. Ed.*, 2005, **44**, 5992–5997; (*c*) Z. Jin, B. Xu and G. B. Hammond, *Tetrahedron Lett.*, 2011, **52**, 1956–1959; (*d*) Y. Zhang, L. Pan, Y. Zou, X. Xu and Q. Liu, *Chem. Commun.*, 2014, **50**, 14334–14337; (*e*) H. Yu, Y. Chen and Y. Zhang, *Chin. J. Chem.*, 2015, **33**, 531–534; (*f*) C. Mei, Y. Hu and W. Lu, *Synthesis*, 2018, 2999–3005; (*g*) H.-H. Chang, X.-X. He, Z.-L. Zang, C.-H. Zhou and G.-X. Cai, *Asian J. Org. Chem.*, 2022, **11**, e202200500; (*h*) N. Neerathilingam and R. Anandan, *RSC Adv.*, 2022, **12**, 8368–8373; (*i*) S.-H. Liu, Z.-C. Dong, Z.-L. Zang, C.-H. Zhou and G.-X. Cai, *Org. Biomol. Chem.*, 2024, **22**, 1205–1212; (*j*) C. Gu, T. Yatabe, K. Yamaguchi and K. Suzuki, *Chem. Commun.*, 2024, **60**, 4906–4909; (*k*) J. Qi, X. Wang, G. Wang, S. R. Dubbaka, P. O'Neill, H. T. Ang and J. Wu, *Green Chem.*, 2024, **26**, 306–311.
10 (*a*) X. Ye, C. Xie, Y. Pan, L. Han and T. Xie, *Org. Lett.*, 2010, **12**, 4240–4243; (*b*) T. Brandhofer, A. Gini, S. Stockerl, D. G. Piekarski and O. G. Mancheno, *J. Org. Chem.*, 2019, **84**, 12992–13002; (*c*) B. Wang, D. He, B. Ren and T. Yao, *Chem. Commun.*, 2020, **56**, 900–903; (*d*) T.-T. Xu, Y. Xiao, J.-L. Zhou, L. Tang, F. Wu, J.-Y.-H. Sheng, W.-B. Wu and J.-J. Feng, *Org. Chem. Front.*, 2023, **10**, 4381–4387.
11 (*a*) Y.-Y. Cheng, T. Lei, L. Su, X. Fan, B. Chen, C.-H. Tung and L.-Z. Wu, *Org. Lett.*, 2019, **21**, 8789–8794; (*b*) B.-G. Cai, W.-Z. Yao, L. Li and J. Xuan, *Org. Lett*, 2022, **24**, 6647–6652; (*c*) R. Ma, Y. Ren, Z. Deng, K.-H. Wang, J. Wang, D. Huang, X. Lv and Y. Hu, *Org. Lett.*, 2023, **25**, 4080–4085; (*d*) M. Hitt, A. Norris and A. N. Vedernikov, *Org. Lett.*, 2023, **25**, 5504–5508.
12 (*a*) X. Zhang, T. Cui, X. Zhao, P. Liu and P. Sun, *Angew. Chem., Int. Ed.*, 2019, **132**, 3493–3497; (*b*) Q. Chu, Z. Feng, S. Zhang, P. Liu and P. Sun, *Green Chem.*, 2023, **25**, 6728–6732; (*c*) W. Zhou, P. Chen, Z.-Q. Li, L.-T. Xiao, J. Bai, X.-R. Song, M.-J. Luo and Q. Xiao, *Org. Lett.*, 2023,

25, 6919–6924; (*d*) P. Jiang, C. Liang, T. He, R. Liu, X. Meng, Y. Zheng and S. Huang, *Eur. J. Org. Chem.*, 2024, e202400469.
13 (*a*) D. A. Evans, P. Nagorny and R. Xu, *Org. Lett.*, 2006, **8**, 5669–5671; (*b*) T. Tomizawa, K. Orimoto, T. Niwa and M. Nakada, *Org. Lett.*, 2012, **14**, 6294–6297; (*c*) Y. Shen, Q. Li, G. Xu and S. Cui, *Org. Lett.*, 2018, **20**, 5194–5197; (*d*) J.-L. Xu, H. Tian, J.-H. Kang, W.-X. Kang, W. Sun, R. Sun, Y.-M. Li and M. Sun, *Org. Lett.*, 2020, **22**, 6739–6743; (*e*) X. Du, D. Xu, G. Xu, C. Yu and X. Jiang, *Org. Lett.*, 2022, **24**, 7323–7327.
14 (*a*) R. Ballini, G. Bosica, D. Fiorini and M. Petrini, *Tetrahedron Lett.*, 2002, **43**, 5233–5235; (*b*) S. Umemiya, K. Nishino, I. Sato and Y. Hayashi, *Chem. – Eur. J.*, 2014, **20**, 15753–15759.
15 J. Li, M. J. Lear and Y. Hayashi, *Angew. Chem., Int. Ed.*, 2016, **55**, 9060–9064.
16 (*a*) S. Swetha and G. C. Senadi, *Adv. Synth. Catal.*, 2022, **364**, 2872–2882; (*b*) S. Sathyendran, K. Muthu, K. Govindan, N.-Q. Chen, W.-Y. Lin and G. C. Senadi, *Org. Lett.*, 2023, **25**, 4086–4091; (*c*) S. Sathyendran and G. C. Senadi, *Asian J. Org. Chem.*, 2023, **12**, e202300433; (*d*) J.-P. Leblanc and H. W. Gibson, *J. Org. Chem.*, 1994, **59**, 1072–1077.
17 L. Capaldo, Z. Wen and T. Noël, *Chem. Sci.*, 2023, **14**, 4230–4247.
18 W. Li, S. Li, L. Luo, Y. Ge, J. Xu, X. Zheng, M. Yuan, R. Li, H. Chen and H. Fu, *Green Chem.*, 2021, **23**, 3649–3655.